X-RAY STUDY OF BILAYER TILTED STRUCTURES FOR SIDE-CHAIN LIQUID CRYSTAL POLYMERS

B. I. OSTROVSKII[1], E. A. SOTO BUSTAMANTE[2], S. N. SULIANOV[1], YU. G. GALYAMETDINOV[3] and W. H. HAASE[2]

[1]*Institute of Crystallography, Academy of Sciences of Russia, Leninsky pr. 59, Moscow 117333, Russia*

[2]*Institut fur Physikalische Chemie, Technische Hochschule Darmstadt, Petersenstrase 20, 64287 Darmstadt, Germany*

[3]*Kazan Physico Technical Institute, Sibirsky Tract 10/7, 420029, Kazan, Russia*

Structural investigations using X-ray diffraction on methacrylate and acrylate based polymers with different side-chain mesogenic units are presented. The measurements were carried out by means of diffractometers with one and two-coordinate proportional chambers. The bilayer tilted smectic C_2 phase was identified in all of polymers. The structural models bearing the regular alternation of the direction of tilt for side-chains in bilayers are discussed in connection with possible polar (ferroelectric) or antiferroelectric behaviour of achiral mesogenic polymers. The results of repolarization experiments are discussed.

INTRODUCTION

In recent years there have been made considerable efforts, both experimental[1-3] and theoretical[4-8], in a search for novel structures among achiral liquid crystals possessing polar (ferroelectric) or antiferroelectric order. One interesting possibility here is connected with remarkable symmetry properties of so called "chevron" smectic phases[9,10] in which the direction of tilt regularly alternates from one layer to another, Figure 1. Such smectic phases were known to exist for a long time[11-15], however the increasing activity in this field was stimulated by a discovery in 1989 of the antiferroelectric behaviour for some chiral smectics with alternating layer to layer tilt[16]. The chevron smectic C phase in achiral systems is nonpolar due to the up-down symmetry in orientation of long molecular axes and vertical mirror plane, Figure 1a. However in the presence of the chain backbone for polymer mesogens or solvent for lyotropic liquid crystals the up-down orientational symmetry is broken, resulting in an appearance of polar axes in the plane of smectic layers, Figures 1b, c. Note that in contrast to ferroelectric states of the conventional tilted smectic phases of chiral molecules where the vector of polarization **P** is perpendicular to the plane of tilt[17], in achiral mesogens **P** is lying in the chevron plane.

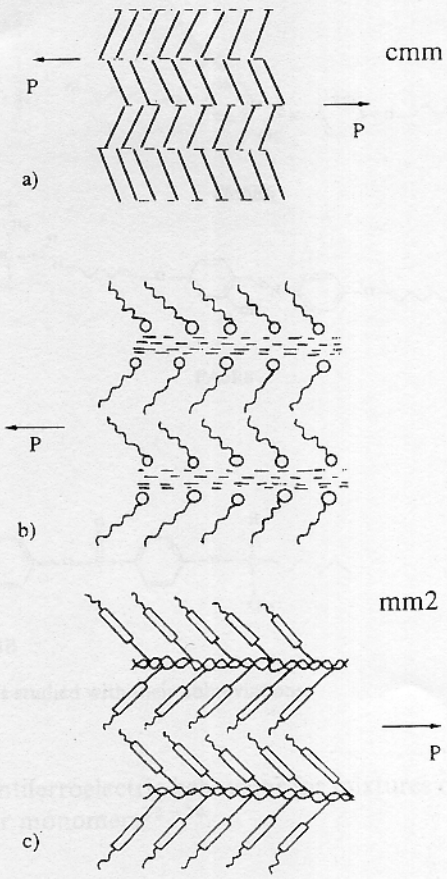

Figure 1 Schematic representation of different types of chevron structures and their symmetry for low molecular mass thermotropic mesogens (a), liotropic systems (b) and side-chain polymer smectics (c).

In order to observe the in-plane polar behaviour for achiral polymer mesogens, two necessary conditions should be satisfied. The first is the bilayer character of one-dimensional periodicity (the layer spacing is of the order of twice of the length of mesogenic units, Fig. 1c). The second is the opposite direction of tilt for the side-chain units of the neighbour main chains. These properties are determined by the molecular architecture of a comb-like polymer, where the mesogenic side-chains with functional groups are attached to the chain backbone via flexible spacers. In order to search for the tilted phases satisfying the aforesaid conditions and hence being good model objects for observation of the new type of polar behaviour, we initiated the structure investigations of a new series of side chain mesogenic polymers. Our study was stimulated by the X-ray and electroptical evidence for bilayer smectic C_2 layering[14,18–21] and chevron structure[22] for some mesogenic polymers. The bilayer smectic C_2 phase was found for a number of polymers under study and their mixtures with corresponding monomers. The pyro- and piezoelectric measure-

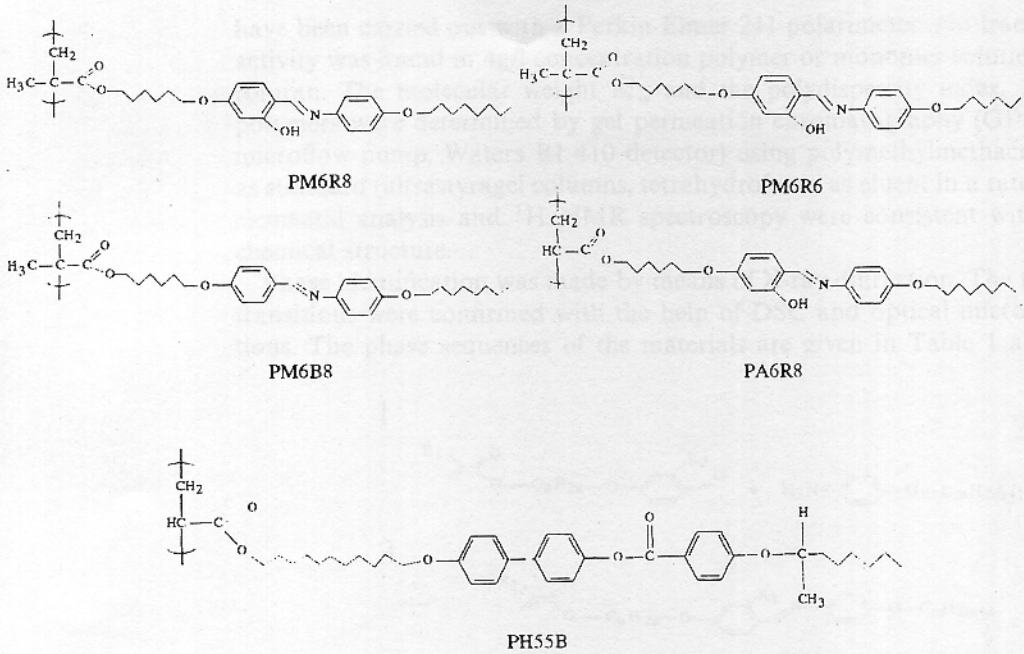

Figure 2 Chemical structures of the polymers studied with their abbreviations.

ments performed in parallel confirmed the antiferroelectric behaviour for mixtures of some of the investigated polymers with their monomers[23-24].

EXPERIMENTAL

The polyacrylate (PA) and polymethacrylate (PM) based mesogenic polymers studied in this work are shown in Figure 2 below. The first and second numbers in the compound abbreviations denote the number of carbon atoms in linear hydrocarbon chains attached to the backbone and outer phenyl ring respectively. The only difference between PM6R8 and PM6B8 mesogens is the absence of hydroxy (salicylidene) group in the side-chain unit of the latter compound.

The preparation of the monomers was carried out by refluxing an ethanolic solution of proper aniline and aldehyde in presence of catalytic amount of hydroquinone (HQ) for 2 hours. After two recrystallizations from methanol, pale yellow plates of a monomer were obtained with 70% yield. The methacrylate polymers were synthesized by radical polymerization of the corresponding monomers in toluene in a sealed vial degased with nitrogen for 72 hours at 60 °C, using α, α′-bis-azoisobutyronitrile (AIBN) as initiator (see reaction scheme in Fig. 3). Subsequent precipitations of the swollen polymers with methanol from concentrated toluene solutions gave the yellow products with 70–80% yield. To prove the achiral nature of polymers under study the measurements of the optical rotatory power

have been carried out with a Perkin-Elmer 241 polarimeter. No trace of the optical activity was found in 4g/l concentration polymer or monomer solutions in tetrahydrofuran. The molecular weight $\bar{M}_w$ and the polydispersity index, $\bar{M}_w/\bar{M}_n$ for the polymers were determined by gel permeation chromatography (GPC) (Waters 510 microflow pump, Waters RI 410 detector) using polymethylmethacrylate (PMMA) as standard (ultrastyragel columns, tetrahydrofuran as eluent in a rate 1ml/min). The elemental analysis and ^{1}H NMR spectroscopy were consistent with the expected chemical structure.

Phase identification was made by means of X-ray diffraction. The temperatures of transitions were confirmed with the help of DSC and optical microscopy observations. The phase sequences of the materials are given in Table 1 along with their

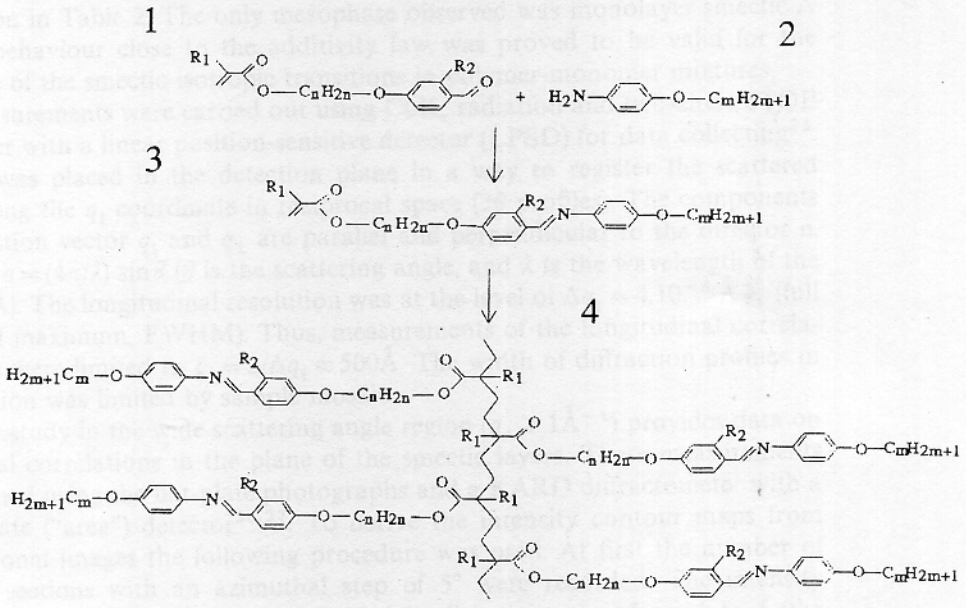

Figure 3 Reaction scheme for preparing of the polymers under study.

Table 1. Phase, transition temperatures [°C] and some polymer and liquid crystalline characteristics for materials under study; *g* stands for glassy state, *I* for isotropic liquid, *A* and *C* for different types of smectic phases; (*) racemic mixture

Polymer	Phase behaviour	$(\bar{M}_w)$	$(\bar{M}_w/\bar{M}_n)$	P_g	L, Å	d_2 Å	d_2/L
PM6B8	*g*-80-C_2-161-*I*	64.500	1.9	130	33	54	1.64
PM6R8	*g*-93-C_2-184-*I*	81.500	2.1	160	33	51	1.55
PM6R6	*g*-82-C_2-157-A_d-173-*I*	54.300	2.4		31	50	1.61
PA6R8	*g*-60-C_2-180-*I*	85.200	5.8	168	33	55	1.67
PH55B(*)	*g*-60-C_x-115-C_2-150-*I*			180	43	68	1.58

molecular masses, dispersion indices, degrees of polymerization (P_g), the lengths of the monomeric (side-chain) units (L), layer spacing in the bilayer smectic C_2 phase (d_2) and ratio d_2/L.

Note that the last polymer mesogen in Table 1 (PH55B) in its enantiotropic form was studied earlier using X-ray diffraction[19] and electrooptic[21] technique. It was shown that it has bilayer tilted structure and "butterfly"-like optical transmittance hysteresis curve that are characteristic of an antiferroelectric state in conventional chiral substances. This means that PH55B has local structure of the type presented on Figure 1c. The racemic mixture of this mesogen kindly provided to us by Dr R. Zentel (Mainz) was considered as a convenient model object for detection of the in-plane polarization effects described above.

The transition temperatures and molecular length of the corresponding monomers are given in Table 2. The only mesophase observed was monolayer smectic A phase. The behaviour close to the additivity law was proved to be valid for the temperatures of the smectic-isotropic transitions in polymer-monomer mixtures.

X-ray measurements were carried out using CuK_α radiation and two-circle STOE diffractometer with a linear position-sensitive detector (LPSD) for data collecting[25]. The LPSD was placed in the detection plane in a way to register the scattered radiation along the $q_\parallel$ coordinate in reciprocal space (2θ profiles). The components of the diffraction vector $q_\parallel$ and $q_\perp$ are parallel and perpendicular to the director $\mathbf{n}$, respectively: $q = (4\pi/\lambda)\sin\theta$ (θ is the scattering angle, and λ is the wavelength of the X-rays, 1.54Å). The longitudinal resolution was at the level of $\Delta q_\parallel = 4.10^{-3}$ Å^{-1} (full width at half maximum, FWHM). Thus, measurements of the longitudinal correlations lengths were limited to $\xi_\parallel = 2/\Delta q_\parallel \approx 500$Å. The width of diffraction profiles in the $q_\perp$ direction was limited by sample mosaic.

The X-ray study in the wide scattering angle region ($q_\perp \geqslant 1$Å^{-1}) provides data on the positional correlations in the plane of the smectic layers. These measurements were performed using the flat-plate photographs and a KARD diffractometer with a two-coordinate ("area") detector[26,27]. To derive the intensity contour maps from two dimensional images the following procedure was used. At first the number of radial cross-sections with an azimuthal step of 5° were recorded. The intensity distribution in each cross-section was divided in discrete groups from 1 to 4 (the maximum intensity was set equal to 4). In this way the contours of equal intensity in gradations 1, 2, 3 were displayed.

Diffraction patterns were recorded both from powder specimens (on polymers placed in thin-walled glass capillaries) and from well aligned samples. Alignment of polymer mesogens, as compared to low molar mass liquid crystals, is more difficult.

Table 2. Phases, transition temperatures [°C] and molecular length L[Å] for investigated monomers

Monomer	Phase behaviour	L
M6R8	K-54-A-96-I	33
M6R8	K-63-A-95-I	31
M6B8	K-71-A-114-I	33
M6R8	K-59-A-119-I	32

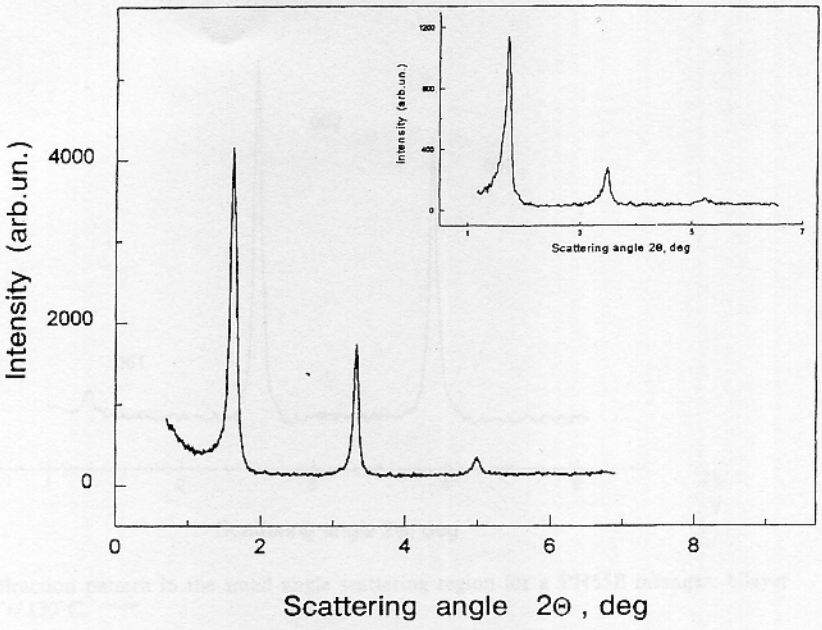

Figure 4 X-ray diffraction pattern in the small angle scattering region for a PM6R8-M6R8 (74:26) mixture; bilayer smectic C_2 phase, $T = 120°C$. The inset shows the same type of pattern for pure PM6R8 mesogen.

Our first attempts to align samples in 1T strength magnetic field were unsuccessful. Therefore oriented films were prepared using shear aligning technique. The polymer was placed between glass plates and heated to the temperature close to the transition into isotropic liquid. Then to provide a shear the cover glass was repeatedly (and circularly) moved relative to the substrate. After quenching to room temperature the oriented textures with smectic planes parallel to the film surface were memorized. The thickness of the films was typically about 50–100μm.

RESULTS AND INTERPRETATION

The X-ray patterns of the compounds under study below isotropic transition exhibit sharp inner reflections and diffuse outer halos. Obviously, these reflect the smectic character of mesophases. The inner reflections are a set of 00n resolution limited peaks at $q_n = 2\pi n/d$, where n is an integer ($n = 1-3$) and d is the layer spacing, Figures 4, 5. There is a systematic difference in the ratio of the intensity of second to first harmonic for pure polymers and their mixtures with monomers ($I_2/I_1 \approx 20\%$ and $I_2/I_1 \approx 40\%$ for pure PM6R8 and its 33%mixture, respectively, $T = 90°C$). These reflect changes in the distribution of the electron density in the direction along layer normal with admixing monomers. In some extreme cases, as it happens to PH55B mesogen, the intensity of higher order peaks is even larger than

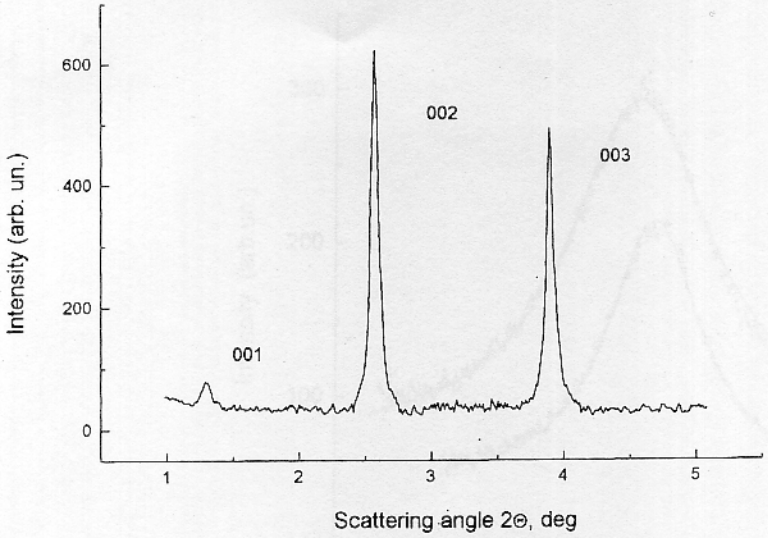

Figure 5 X-ray diffraction pattern in the small angle scattering region for a PH55B mesogen; bilayer smectic C_2 phase, $T = 130°C$.

the first harmonic, Figure 5. The same X-ray picture was observed earlier for the enantiotropic form of PH55B[19].

It should be emphasized that in mixtures under study (at least, up to 33% concentration of monomers) the X-ray diffraction in smectic phases revealed one set of 00n reflections, which is characteristic of a uniform (ideal mixing) state. X-ray measurements do not reveal any broadening of 00n peaks or any additional diffuse scattering with admixing monomers. It means that monomers randomly occupy bilayers formed by a polymer matrix. No indication was found of segregation of the components of a mixture into alternating layers within the same phase or of phase separation. With time, subtle crystalline reflexes, which were proved to belong to crystallization of monomer dopants, were observed in glassy state. However, the smectic ordering in polymer-monomer mixtures preserved at room temperatures at least for several months.

The diffuse outer peaks centered at $q_\perp \approx 1.4\text{Å}^{-1}$ ($2\theta \approx 20$ deg.), corresponds to the average intermolecular distances 4.3-4.5Å within the smectic planes, Figure 6. These peaks are well fitted by the Lorentzian line shapes (solid lines). The corresponding in-plane correlation length $\xi_\perp$, inversely proportional to the peak width, is of the order of 6-10Å. Thus a molecular packing within the smectic layers may be considered as liquid-like. It should be noted that for polymer-monomer mixture the in-plane correlation length is 1.5 times less than in pure monomer ($\xi_\perp = 6$Å and 9Å for 74:26 PM6R8-M6R8 mixture and pure PM6B8 polymer, respectively, Fig. 6). It means that admixing monomers to mesogenic polymer matrix slightly impairs short-range in-plane positional order.

The temperature variations of the layer spacing for a number of polymer mesogens and their mixtures with corresponding monomers are shown in Figures. 7, 8.

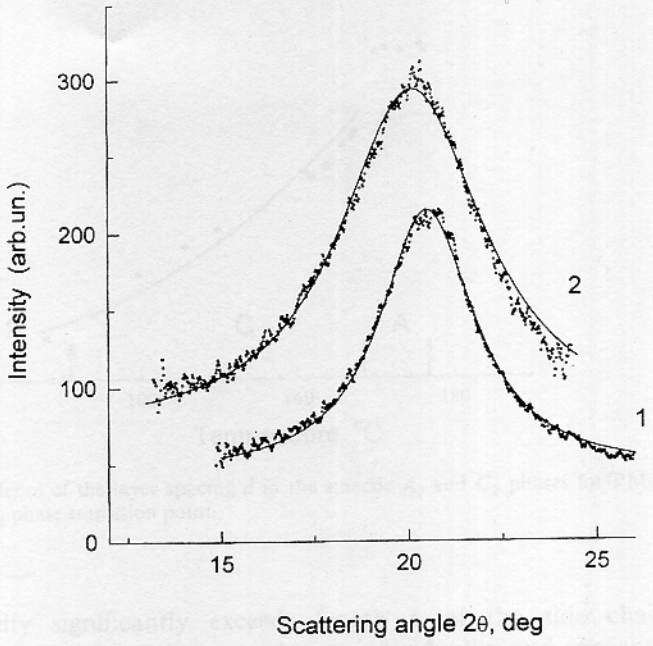

Figure 6 A cross-section of the diffuse outer peaks, taken with an area detector, showing liquid-like in-plane order. 1. PM6B8 mesogen; 2. PM6R8-M6R8 (74:26) mixture.

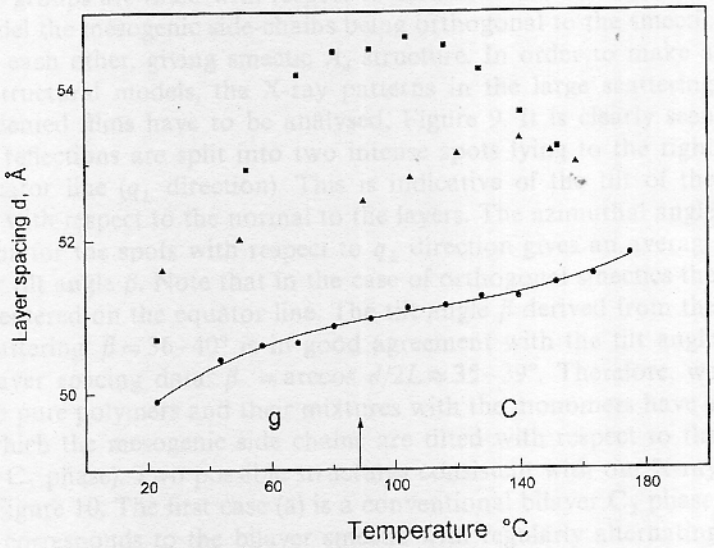

Figure 7 Temperature dependences of the layer spacing in the smectic C_2 phase for PM6R8 mesogen (circles and solid line), PM6R8-M6R8 (74:26) mixture (triangles) and PM6R8-M6R8 (67:33) mixture (squares).

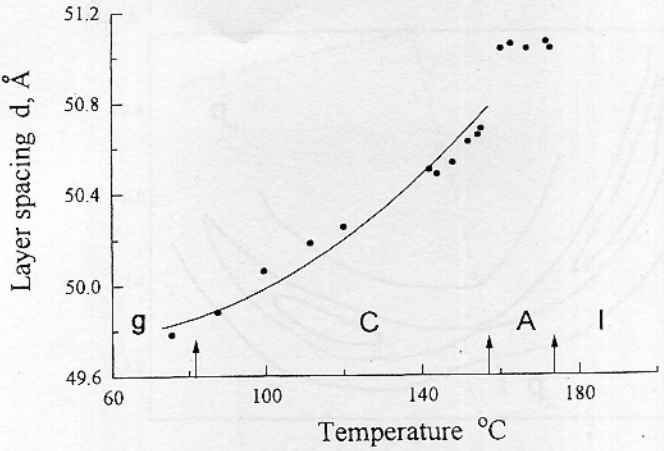

Figure 8 Temperature dependence of the layer spacing d in the smectic A_d and C_2 phases for PM6R6 mesogen. Arrow indicate A_d-C_2 phase transition point.

The interlayer periodicity significantly exceeds length L of the side chains: $d/L = 1.5–1.7$ in dependence on temperature, polymer individuality and concentration of monomers in the mixtures, Table 1 (for example, the fully extended length of a side-chain mesogenic unit plus a backbone segment was estimated from a stereomodel to be $L = 33 \pm 1$Å for PM6R8). This implies some form of bilayer arrangement of side-chain mesogenic units in smectic planes. We can assume bilayer structure in which side groups are tilted with respect to the normal to the layers. In another structural model the mesogenic side-chains being orthogonal to the smectic planes, partly overlap each other, giving smectic A_d structure. In order to make a choice between two structural models, the X-ray patterns in the large scattering angles region from oriented films have to be analysed, Figure 9. It is clearly seen that the outer diffuse reflections are split into two intense spots lying to the right and left from the equator line ($q_\perp$ direction). This is indicative of the tilt of the mesogenic side-chains with respect to the normal to the layers. The azimuthal angle of the intensity maxima for the spots with respect to $q_\perp$ direction gives an average value of the molecular tilt angle β. Note that in the case of orthogonal smectics the outer reflections are centered on the equator line. The tilt angle β derived from the geometry of X-ray scattering: $\beta = 36–40°$ is in good agreement with the tilt angle calculated from the layer spacing data: $\beta = \arccos d/2L \approx 35–39°$. Therefore, we conclude that both the pure polymers and their mixtures with the monomers have a bilayer structure in which the mesogenic side chains are tilted with respect to the layer normal (smectic C_2 phase). Two possible structures consistent with our X-ray data are sketched in Figure 10. The first case (a) is a conventional bilayer C_2 phase, the second model (b) corresponds to the bilayer smectic with regularly alternating direction of the tilt (chevron structure). Because of the liquid-like order in smectic layers it seems impossible to make a choice between the structures of the type of Figure 10a and Figure 10b by X-ray diffraction only. On the first sight the projec-

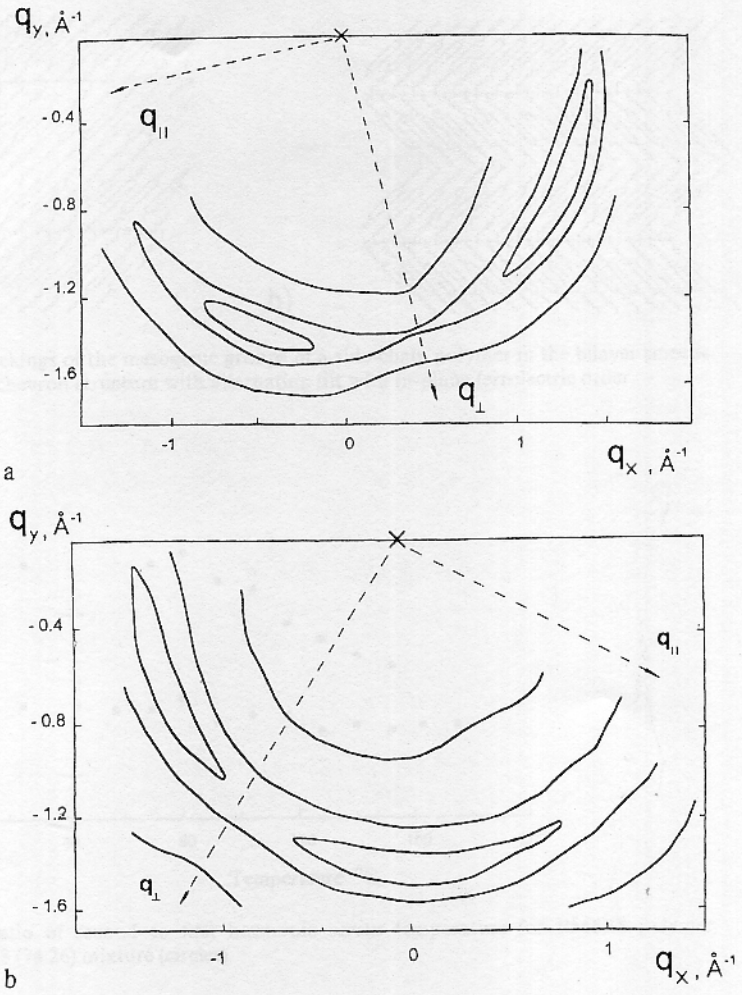

Figure 9 X-ray diffraction patterns in a wide scattering angles region for PM6B8 mesogen (a) and PM6R8-M6R8-74:26 mixture (b). Frozen bilayer smectic C_2 phase. Q_x and q_y are the coordinates of the area detector, the components of the scattering wave vector $q_\parallel$ and $q_\perp$ lie along layer normals and in the plane of smectic layers respectively. The small angle peaks shown in Figure. 4 are omitted for the intensity scale difference.

tions of electron density distribution function on the layer normal direction in both cases are the same. However in the presence of specific intermolecular interaction stabilizing the chevron ordering, density distribution function may be somewhat different from that in conventional tilted structures, resulting in changes of relative intensity of small angle diffraction peaks from layer structure [28]. These changes may point to the transformation of conventional tilted structure to chevron structure as discussed below.

In the smectic C_2 phases for pure polymers PM6R8, PM6B8 and PA6R8 the layer spacing d slightly decreases with decreasing temperature. This behaviour is typical of

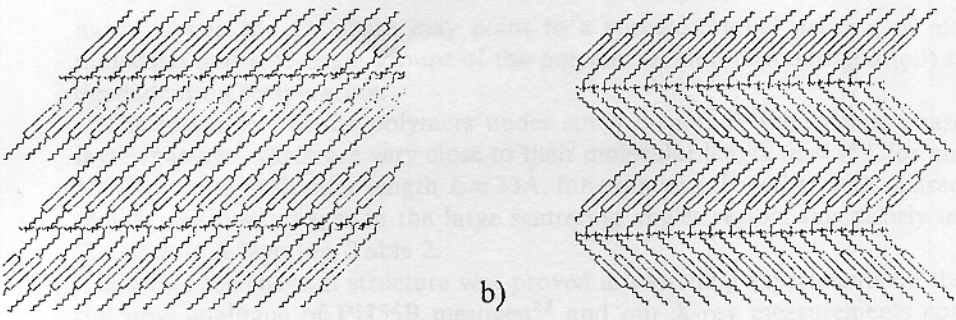

Figure 10 Two possible packings of the mesogenic groups of a side-chain polymer in the bilayer smectic C_2 phase: a) uniform tilt; b) chevron structure with alternating tilt with in-plane ferrolectric order.

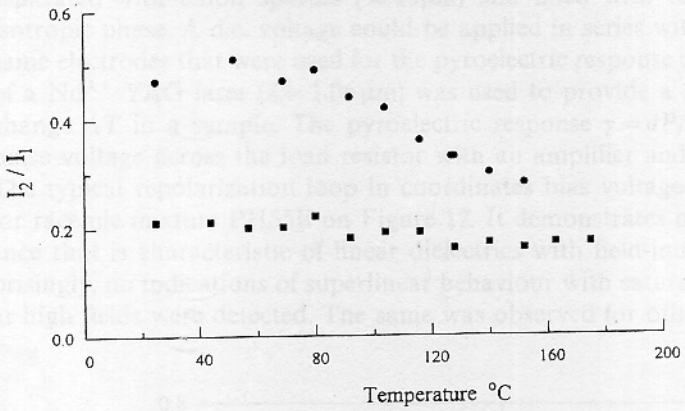

Figure 11 The intensity ratio of second to first harmonic *versus* temperature for PM6R8 polymer (squares) and PM6R8-M6R8 (74:26) mixture (circles).

the strong first order phase transitions from the isotropic to tilted phases associated with a large jump in tilt angle at the phase transition point. With further decreasing temperature the tilt angle only slightly increases. On the other hand for PM6R6 polymer which has high temperature smectic A_d phase the temperature variations of d display a fracture at the $A_d \Leftrightarrow C_2$ phase transition point, which is characteristic of phase transitions between orthogonal and tilted smectic phases, Figure 8. The d values in C_2 phase for polymers doped with their monomers are systematically larger than in pure polymer, moreover, the layer periodicity displays an unusual nonmonotonic temperature dependence, Figure 6. For example, for a mixture containing 33% of monomer, interlayer spacing firstly increases in the range of 160–100°C (from 53 to 54.7Å) then, in the range of 100–25°C, decreases (down to 51Å in the glassy state). The temperature variation of the intensity ratio of first two harmonics for the same mixture correlates with the $d(T)$ dependence, Figure 11. The anomalous behaviour of the spacing and the relative intensities of successive

harmonics in the C_2 phase may point to a specific mutual packing of monomer molecules and side-chain groups of the polymer (a kind of interdigitation) strongly dependent on temperature.

The monomers of the polymers under study display in the smectic phase interlayer spacings, which are very close to their molecular length ($d = 35$Å for monomer M6R8 having molecular length $L \approx 33$Å, for example). Together with characteristic two-dimensional images in the large scattering angles region, this clearly indicates the smectic A layering, Table 2.

Because the chevron structure was proved in switching experiments on the enantiotropic analogue of PH55B mesogen[22] and our X-ray measurements confirmed bilayer character of its periodicity, the first attempts to detect the in-plane polarization were performed on racemic mixture of PH55B compound. We have tested the presence of macroscopic polarization of the substance using a pulse pyroelectric technique[29]. The cells were prepared from two nontreated ITO covered glass plates separated with teflon spacers ($\approx 15\mu$m) and filled with the liquid crystal in the isotropic phase. A d.c. voltage could be applied in series with a load resistor to the same electrodes that were used for the pyroelectric response detection. A 100μs pulse of a Nd^{3+} YAG laser ($\lambda = 1.06\,\mu$m) was used to provide a small local temperature change ΔT in a sample. The pyroelectric response $\gamma = dP/dT$ was measured as a pulse voltage across the load resistor with an amplifier and a storage oscilloscope. The typical repolarization loop in coordinates bias voltage-pyroresponse is shown for racemic mixture PH55B on Figure 12. It demonstrates near linear field dependence that is characteristic of linear dielectrics with field-induced polarization. Surprisingly, no indications of superlinear behaviour with saturation of the polarization at high fields were detected. The same was observed for other pure polymers under

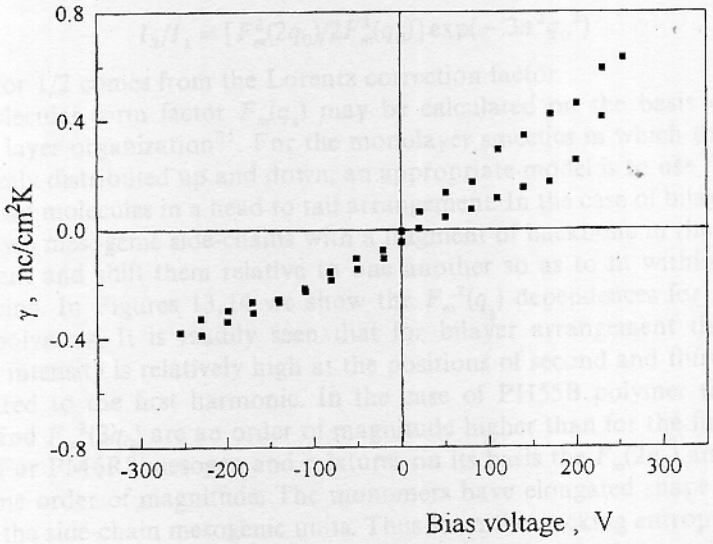

Figure 12 Quasi-static repolarization loop in the coordinates d.c. bias voltage-pyroelectric coefficient obtained for PH55B racemic mixture, $T = 120$°C.

study. In contrast to pure polymer mesogens, some of the mixtures with monomers show typical antiferroelectric loops corresponding to three stable states: one with zero polarization in the absence of the field, and two states with the macroscopic polarization oriented along two possible directions of the external field. The saturation of polarization was observed in the fields about 8V/μm. The details of these experiments will be the subject of special paper[24].

DISCUSSION

In this section we try to relate the peculiarities of the X-ray diffraction observed for polymers under study with a local structure of tilted bilayers. Within instrumental resolution ($\xi_\parallel \leqslant 500$Å), smectic phases in our experiments show long-range translational order. Therefore, diffraction intensity in the direction parallel to the layer normals (z axis or $q_z = q_\parallel$) may be represented in the form [30,31]

$$I(q_z) = F_m^2(q_z) f^2(q_z) \sum \delta(q_z - q_n) * \sin^2(Rq_z/2)/(q_z/2)^2 \qquad (1)$$

where molecular form factor $F_m(q_z)$ is the Fourier transform of the z projection of the electron density profile of molecule (side-chain) averaged in accordance with local distribution of molecules in the layers; $f(q_z)$ is the Fourier transform of the molecular centre of mass distribution $f(z)$ within the layer: $f(q_z) \sim \exp(-\sigma^2 q_z^2)$, the width of the Gaussian distribution function σ mainly depends on the mean square amplitude of the layer displacements u in the direction along the layer normal: $\sigma^2 = \langle u^2(r) \rangle$; R is of the order of $\xi_\parallel$, and the asterisk denotes the convolution operation. According to equation (1), the intensities of high-order reflections are reduced by a factor $\exp(-\sigma^2 q_z^2)$ analogous to the Debye-Waller factor for crystals. The ratio of intensities of two successive harmonics is given by:

$$I_2/I_1 = [F_m^2(2q_0)/2F_m^2(q_0)] \exp(-3\sigma^2 q_0^2) \qquad (2)$$

where factor 1/2 comes from the Lorentz correction factor.

The molecular form factor $F_m(q_z)$ may be calculated on the basis of a certain model for layer organization[31]. For the monolayer smectics in which the molecules are randomly distributed up and down, an appropriate model is to use the z coordinates for two molecules in a head to tail arrangement. In the case of bilayer smectics, we place two mesogenic side-chains with a fragment of backbone in the antiparallel arrangement and shift them relative to one another so as to fit within the known layer spacing. In Figures 13, 14 we show the $F_m^2(q_\parallel)$ dependences for PH55B and PM6R8 polymers. It is readily seen that for bilayer arrangement the molecular scattering intensity is relatively high at the positions of second and third harmonics as compared to the first harmonic. In the case of PH55B polymer the values of $F_m^2(2q_0)$ and $F_m^2(3q_0)$ are an order of magnitude higher than for the first harmonic $F_m^2(q_0)$. For PM6R8 mesogen and mixtures on its basis the $F_m(2q_0)$ and $F_m(q_0)$ are of the same order of magnitude. The monomers have elongated shape of the same length as the side-chain mesogenic units. Thus from the packing entropy standpoint it is more probable for monomers to lie parallel the side-chain units especially taking into account the presence of numerous vacancies along the main chain

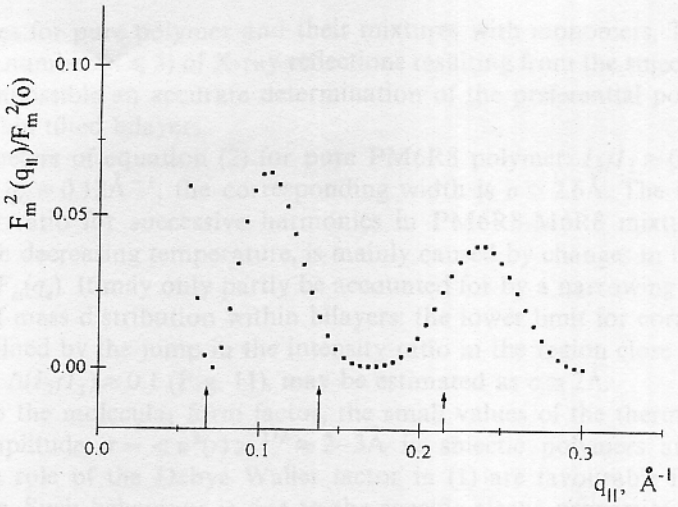

Figure 13 The wavelength ($q_{||}$) dependence of the square of the molecular formfactor (normalized to the $F_m^2(0)$ values) calculated for PH55B mesogen; arrows indicate positions of successive harmonics.

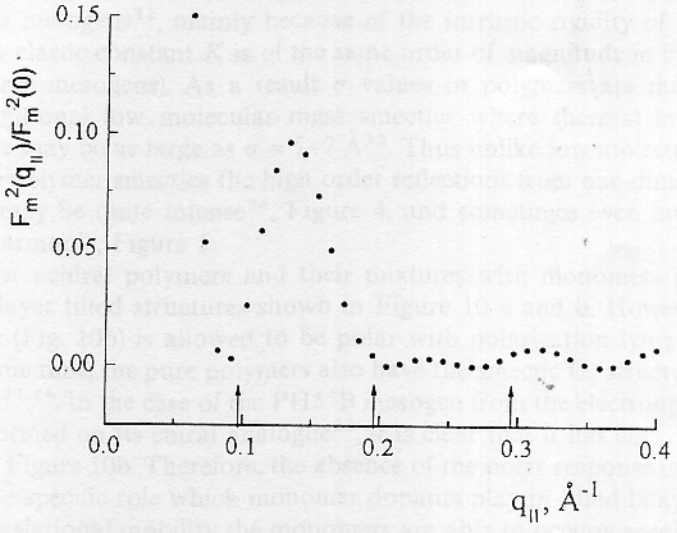

Figure 14 The F_m^2 ($q_{||}$) dependence calculated for PM6R8 polymer; the designations are the same as in the Figure 13.

caused by the statistical character of arrangement of side-chains relative to the backbone units. Because of the high translational mobility of the monomers, they are able to occupy specific positions relative to the side-chain units, thus providing additional interaction in the system which may stabilize the chevron ordering. Because of the similar distribution of electron density in monomers and in side-chain mesogenic groups the molecular formfactor calculations give near the same

wavelength dependences for pure polymer and their mixtures with monomers. Together with the limited number ($n \leqslant 3$) of X-ray reflections resulting from the smectic layering, this makes impossible an accurate determination of the preferential positions of monomers within tilted bilayers.

For values of parameters of equation (2) for pure PM6R8 polymer: $I_2/I_1 \approx 0.2$, $F_m^2(2q_0)/F_m^2(q_0) \approx 0.5$, $q_0 = 0.12\text{Å}^{-1}$, the corresponding width is $\sigma \cong 2.6\text{Å}$. The increase in the intensity ratio for successive harmonics in PM6R8-M6R8 mixture (33% of monomer) with decreasing temperature, is mainly caused by changes in the molecular form factor $F_m(q_z)$. It may only partly be accounted for by a narrowing of the molecular centre of mass distribution within bilayers: the lower limit for corresponding width determined by the jump in the intensity ratio in the region close to the isotropic transition $\Delta(I_2/I_1) \approx 0.1$ (Fig. 11), may be estimated as $\sigma \cong 2\text{Å}$.

Thus, additionally to the molecular form factor, the small values of the thermal layer displacement amplitude $\sigma = <u^2(r)>^{1/2} \approx 2\text{–}3\text{Å}$ in smectic polymers and hence reduction of the role of the Debye Waller factor in (1) are favourable for higher order harmonics. Such behaviour is due to the specific elastic properties of layered polymer mesogens. The layer displacement amplitude is related to the combination of elastic constants of smectics by the equation: $(\sigma/d)^2 \sim (KB)^{-1/2}$, where B and K are the elastic constants for compression of the layers and for splay deformation, respectively[30]. The B values are much larger for polymer smectics as compared to low molecular mass mesogens[32], mainly because of the intrinsic rigidity of the backbone chains (splay elastic constant K is of the same order of magnitude in high and low molecular mass mesogens). As a result σ values in polymers are much smaller than in conventional low molecular mass smectics where thermal layer displacement amplitude may be as large as $\sigma = 5\text{–}7\ \text{Å}$[33]. Thus unlike low molecular mass smectics[33], in the polymer smectics the high order reflections from one-dimensional layer structure may be quite intense[34], Figure 4, and sometimes even more intense than the first harmonic, Figure 5.

Our X-ray results for achiral polymers and their mixtures with monomers are consistent with two bilayer tilted structures shown in Figure 10 a and b. However only chevron structure (Fig. 10b) is allowed to be polar with polarization lying in the tilt plane. At the same time, the pure polymers also have the smectic C_2 structure but electrically inactive[23,24]. In the case of the PH55B mesogen from the electrooptical measurements performed on its chiral analogue[22], it is clear that it has chevron structure of the type of Figure 10b. Therefore, the absence of the polar response in it may be indicative of the specific role which monomer dopants play in tilted bilayer matrix: due to high translational mobility the monomers are able to occupy specific positions relative to the side-chain units and thus provide a component of the dipole moment necessary to observe polarization. On the other hand we cannot exclude that the other pure polymers have the conventional structure, shown in Figure 10a and a role of the monomer dopant is to induce the smectic structure with alternating tilt. The role of the monomer additives in provoking new structures has been reported earlier[35].

To prove the chevron character of a tilted structure experimentally, is a very sophisticated trick[28]. In chiral systems with a macroscopic helix it can be made by observing specific features of the optical transmission spectra for light incident

obliquely on to the helical structure. Alternative evidence consists in optical observations of the inversion of tilt and polarization direction in extremely thin smectic films (the thickness of the order of two-six layers)[13,36], or is given by observation of $s = +1/2$ defects in the **c** director field[28]. Our attempts to draw thin free standing films of polymer PH55B proved unsuccessful. At first, because of high viscosity of the polymer even at the temperatures close to isotropic phase, the films were rather thick (more than thirty layers). Secondly, because of an extremely high surface to volume ratio in free standing films the cross-linking reactions (*e.g.* through photo-or thermal oxidation) were so fast that for a time less than one hour the films transit to a rubber state.

It should be emphasized that the structure model presented in Figure 10b principally does not permit antiferroelectricity. Initially the macroscopic polarization is zero due to the presence of azimuthally disordered domains (the system is degenerated in the plane of layers). After applying field, the regions of bilayers with in-plane polarization opposite to the field reorient in the field direction and a macroscopic polarization appear. But after switching the field off domains store their orientation. As a result we have bistability and ferroelectric like repolarization (hysteresis) curve. To explain the antiferroelectric behaviour observed for polymer monomer mixtures the structure have to be locally nonpolar in the off state. The chevron type bilayer structures which satisfies the aforeside conditions are presented in Figure 15. This picture is analogous to structure of chiral antiferroelectrics[28] and corresponds to a double repolarization loop typical of antiferroelectrics.

The maximum magnitude of the macroscopic polarization measured ($400\,nC/cm^2$)[23,24] may be accounted for if we assume that all mesogenic units of both polymer and monomer have their dipole moment projections on the field direction of about 1 Debye which is quite reasonable. On transition to the glassy state a field induced macroscopic polarization becomes frozen and the material

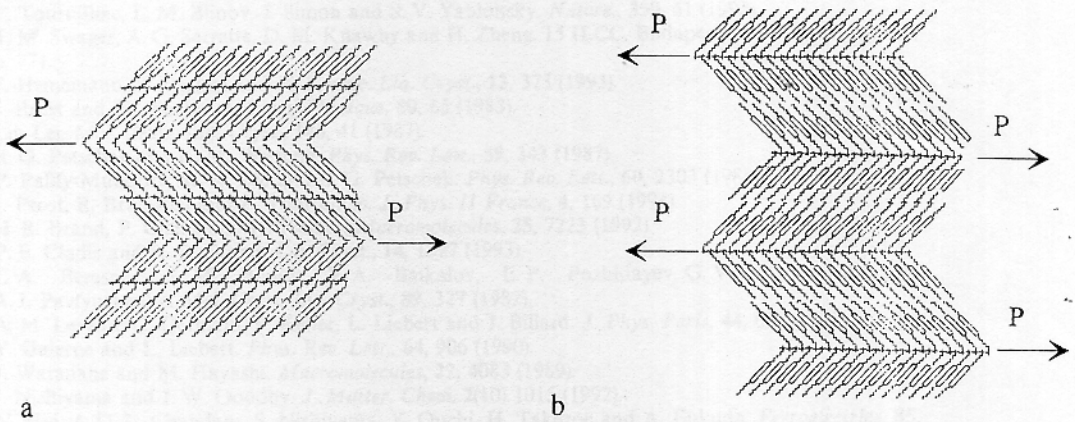

Figure 15 Two possible packings of a side-chain polymer in the bilayer smectic C_2 phase with alternating tilt and in-plane antiferroelectric order; the fracture in the direction of tilt takes place either in the regions of tails (model *a*) or (heads model *b*) of mesogenic groups.

manifest pyroelectric response comparable with those typical of proper polymer ferroelectrics.

The molecular mechanism of the phenomenon remains the subject of speculations. Let us note first, that antiferroelectricity is observed only in the case when both components of a polyer-monomer pair have a hydroxy group no matter whether we deal with acrylate or methacrylate main chain as well as with eight or six carbon atoms in the alkyloxy end tail[23,24]. The absence of the hydroxy group at least in one component of a mixture eliminates antiferroelectricity. In our opinion the hydroxy group may play a double role. On one hand it may be conducive to in-layer polar packing due to dipole-dipole interaction well known from the physics of crystalline ferroelectrics[37]. On the other hand, as soon as antiferroelectric structure with in-plane polarization is established for some other reasons, the hydroxy group may provide a component of the dipole moment necessary for high polarization.

Acknowledgements

The authors are grateful to L. Blinov, P. Cladis, S. Diele, and S. Yablonsky for helpful discussions and Dr. Disselhof of Deutsche Kunstsoff Institute for polymer molar mass determination. We are indebted to R. Zentel for providing us with PH55B compound and useful discussions. Special thanks are due to D. Link and J. Maclennan for the attempts to draw free standing films of PH55B polymer and stimulating discussions. Two of us (B.O. and S.S.) acknowledge financial support from Russian Fund for Fundamental Research (under grant 95–02–03541). We are grateful to Deutsche Telekom for financial support. We also acknowledge the DFG support (AZ 4381/113/112/01) for a bilateral Russian-German cooperation, and the VW support (AZ I/70668) for co-operation with East Europe.

References

1. F. Tournilhac, L. M. Blinov, J. Simon and S. V. Yablonsky. *Nature.*, **359**, 61 (1992).
2. T. M. Swager, A. G. Serrette, D. M. Knawby and H. Zheng. 15 ILCC, Budapest, 1994, Abstracts, V.2, p. 771.
3. S. Heinemann, R. Pashke and H. Kresse. *Liq. Cryst.*, **13**, 373 (1993).
4. J. Prost and Ph. Barois. *J. Chim. Physique*, **80**, 65 (1983).
5. Lin Lei. *Mol. Cryst. Liq. Cryst.*, **146**, 41 (1987).
6. R. G. Petschek and K. M. Wiefling. *Phys. Rev. Lett.*, **59**, 343 (1987).
7. P. Pallfy-Muhoray, M. A. Lee and R. G. Petschek. *Phys. Rev. Lett.*, **60**, 2303 (1988).
8. J. Prost, R. Bruinsma and F. Tournilhac. *J. Phys. II France*, **4**, 169 (1994).
9. H. R. Brand, P. Cladis and H. Pleiner. *Macromolecules*, **25**, 7223 (1992).
10. P. E. Cladis and H. R. Brand. *Liq. Cryst.*, **14**, 1327 (1993).
11. L. A. Beresnev, L. M. Blinov, V. A. Baikalov, E. P. Pozhidayev, G. V. Purvanetskas and A. I. Pavlyuchenko. *Mol. Cryst. Liq. Cryst.*, **89**, 327 (1982).
12. A. M. Levelut, C. Germain, P. Keller, L. Liebert and J. Billard. *J. Phys. Paris*, **44**, 623 (1983).
13. Y. Galerne and L. Liebert. *Phys. Rev. Lett.*, **64**, 906 (1990).
14. J. Watanabe and M. Hayashi. *Macromolecules*, **22**, 4083 (1989).
15. I. Nishiyama and J. W. Goodby. *J. Matter. Chem.* **2**(10) 1015 (1992).
16. N. Hiji, A. D. L. Chandani, S. Nishiyama, Y. Ouchi, H. Takezoe and A. Fukuda. *Ferroelectrics*, **85**, 99 (1988).
17. R. B. Meyer, L. Liebert, L. Strzelecki and P. Keller. *J. Phys. France. Lett.*, **36**, L69 (1975).
18. P. Le Barny and J. C. Dubois. *in Side Chain Liquid Crystal Polymers*, edit. C. B. McArdle (Blackie), 1989, Ch. 5.

19. H. Mensinger and A. Biswas. Polymers for Advanced Technologies, **3**, 257 (1992).
20. O. Francescangeli, B. Yang, E. Chiellini, G. Galli, A. Angeloni and M. Laus. *Liq. Cryst.*, **14**, 981 (1993).
21. J. Enbutt, R. M. Richardson, J. Blackmore, D. G. McDonnell and M. Verrall. *Mol. Cryst. Liq. Cryst.*, **261**, 549 (1995).
22. K. Skarp, G. Andersson, S. T. Lagerwall, H. Kapitza, H. Poths and R. Zental. *Ferroelectrics*, **122**, 127 (1991).
23. E. A. Soto Bustamante, S. V. Yablonskii, L. A. Beresnev, L. M. Blinov, B. I. Ostrovskii and W. Haase. 61. Bunsen-Kolloquium *Ferroelectric Organic Materials in Thin Films*, Darmstadt, February 1996. Abstracts, p.44.
24. E. A. Soto Bustamante, S. V. Yablonskii, B. I. Ostrovskii, L. A. Beresnev, L. M. Blinov and W. Haase. Liq. Cryst. (in press).
25. W. Haase, Z. X. Fan and H. J. Muller. *J. Chem. Phys.*, **89**, 3317 (1988).
26. M. E. Andrianova, D. M. Kheiker and A. N. Popov. *J. Appl. Cryst.*, **15**, 626 (1982); S. N. Sulianov, A. N. Popov and D. M. Kheiker. *J. Appl. Cryst.*, **27**, 934 (1994).
27. L. M. Blinov, T. A. Lobko, B. I. Ostrovskii, S. N. Sulianov and F. G. Tournilchac. *J. Phys. II France*, **3**, 1121 (1993).
28. A. Fukuda, Y. Takanishi, T. Isozaki, K. Ishikava and H. Takezoe. *J. Matter. Chem.*, **4**(7), 997 (1994) and references therein.
29. L. A. Beresnev and L. M. Blinov. *Ferroelectrics*, **33**, 129 (1981).
30. B. I. Ostrovskii. *Liq. Cryst.*, **14**, 131 (1993).
31. T. A. Lobko, B. I. Ostrovskii, A. I. Pavluchenko and S. N. Sulianov. *Liq. Cryst.*, **15**, 361 (1993).
32. E. Nachaliel, E. N. Keller, D. Davidov and C. Boeffel. *Phys. Rev.A.*, **43**, 2897 (1991).
33. P. S. Pershan, *Structures of Liquid Crystal Phases*. World Sci. Lect. Notes in Physics, v.23, World Sci., 1988.
34. P. Davidson and A. M Levelut. *Liq. Cryst.*, **11**, 469 (1992).
35. H. Leube and H Finkelman. *Makromol. Chem.*, **192**, 1317. (1991).
36. Ch. Bahr and D. Fliegner. *Phys. Rev. Lett.*, **70**, 1842 (1993).
37. M. E. Lines and A. M. Glass. *Principles and Applications of Ferroelectrics and Related Materials*. Clarendon Press, Oxford, 1977.